

THE CALCULATION OF BEAM SIZES IN COUPLED ELECTRON STORAGE RINGS

P. Kuske[†], Helmholtz-Zentrum für Materialien und Energie Berlin, Berlin, Germany

Abstract

The description of coupling phenomena in electron storage rings is extended beyond the very common formula based on the coupled Hamiltonian [1] into the region where the small coupling is in competition with damping and diffusion from synchrotron radiation. In the derivation, the moment mapping approach is used in combination with the simplified simulation of radiation effects introduced by Hirata and Ruggiero [2]. The results of this theoretical approach are compared to the predictions of well-established theories dealing with coupling in electron storage rings: The envelope mapping approach from Ohmi, et al. [3], and Chao's SLIM approach [4].

INTRODUCTION

The equilibrium particle distribution in electron storage rings is a result of the balance between diffusion and damping of electrons due to the emission of synchrotron radiation. Linear coupling competes with synchrotron radiation and can create correlations like the tilt of the beam ellipse in the x , and y -plane or an increase of the vertical beam size, however, the coupling has to be strong enough to overcome damping and diffusion. In many 3rd generation light sources, it was found, that the vertical beam size on a nicely compensated linear coupling resonance was much smaller than predicted [5-7]. Figure 1 shows that on the Q_x - Q_y -resonance the vertical beam size is a function of the coupling strength, opposite to the results of the Hamiltonian-based theoretical description of coupling phenomena which predicts a constant vertical beam size once there is a tiny, non-zero coupling, for example, Guignard's or Chao's formula [1, 8]. The lack of a satisfactory explanation has triggered this study.

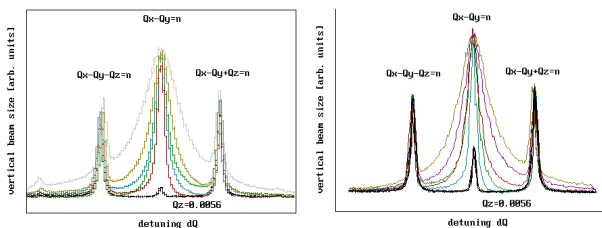


Figure 1: Vertical beam size close to the Q_x - Q_y -coupling resonance for smaller and smaller linear coupling as measured at BESSY II on two different occasions.

A couple of ways are available in the literature to calculate the beam distribution in linearly coupled electron storage rings. In this comparison the focus is on Chao's SLIM approach [4], and the envelope mapping as developed by Ohmi, et al. [3]. We use a simplified mapping approach

based on the modeling of radiation effects as proposed by Hirata and Ruggiero [2].

As long as the beam dynamics in an electron storage ring is linear, the equilibrium distribution of particles will be Gaussian in all dimensions and fully described by the 21 centered second-order moments of the distribution which are the elements of the Σ -matrix. We are interested in measurable quantities like the beam sizes and thus look for the projections of the particle distribution on the coordinate system in the laboratory frame. We are not so much concerned about the normal mode emittances which can be obtained once the Σ -matrix is known [9]. In this comparison the focus is on the coupling created by skew quadrupole magnets, however, this is not restricting the generality of the results.

THEORETICAL APPROACH

In equilibrium between damping and excitation, the Σ -matrix is reproduced turn after turn:

$$\Sigma_{s_0} = R_d \cdot \Sigma_{s_0} \cdot R_d^t + D_{s_0}$$

The damped, and therefore non-symplectic one-turn-matrix at the observation point is denoted by R_d , and its transposed by R_d^t . On average the elements of R_d are slightly smaller than the elements of R due to damping. D_{s_0} is the symmetric diffusion matrix at the observation point, s_0 . In the full envelope mapping approach [3] the calculation of these two matrices requires slicing of all elements where the emission of radiation and coupling takes place. The impact of individual slices on the matrices at the observation point involves an integration around the ring.

Simplified Mapping

We assume that radiation is emitted in dipoles only. Hirata and Ruggiero proposed a simple tracking scheme for particles circulating in a storage ring with radiation [2, 10]. Here a symmetric description in all 6 dimensions is used and we write for the variation of each of the 6 coordinates of the state vector $X = (x, x', y, y', z, \delta)^t$ after one turn:

$$\begin{aligned} x_1 &= (R_{11}x_0 + R_{12}x'_0 + R_{13}y_0 + R_{14}y'_0 + R_{15}z_0 + R_{16}\delta_0)l_x \\ &\quad + R_1 \sqrt{(1-l_x^2)} \cdot \varepsilon_x \cdot \beta_x \\ x'_1 &= (R_{21}x_0 + R_{22}x'_0 + R_{23}y_0 + R_{24}y'_0 + R_{25}z_0 + R_{26}\delta_0)l_x \\ &\quad + R_2 \sqrt{(1-l_x^2)} \cdot \varepsilon_x / \beta_x \\ y_1 &= (R_{31}x_0 + R_{32}x'_0 + R_{33}y_0 + R_{34}y'_0 + R_{35}z_0 + R_{36}\delta_0)l_y \\ &\quad + R_3 \sqrt{(1-l_y^2)} \cdot \varepsilon_y \cdot \beta_y \\ y'_1 &= (R_{41}x_0 + R_{42}x'_0 + R_{43}y_0 + R_{44}y'_0 + R_{45}z_0 + R_{46}\delta_0)l_y \\ &\quad + R_4 \sqrt{(1-l_y^2)} \cdot \varepsilon_y / \beta_y \end{aligned}$$

[†] peter.kuske@helmholtz-berlin.de

$$z_1 = (R_{51}x_0 + R_{52}x'_0 + R_{53}y_0 + R_{54}y'_0 + R_{55}z_0 + R_{56} \delta_0)l_z$$

$$+ R_5 \sqrt{(1-l_z^2)} \cdot \epsilon_z \cdot \beta_z$$

$$\delta_1 = (R_{61}x_0 + R_{62}x'_0 + R_{63}y_0 + R_{64}y'_0 + R_{65}z_0 + R_{66} \delta_0)l_z$$

$$+ R_6 \sqrt{(1-l_z^2)} \cdot \epsilon_z / \beta_z$$

With $l_{x,y,z} = e^{-T_0/\tau_{x,y,z}} \approx 1 - T_0/\tau_{x,y,z}$, where T_0 is the revolution time, and $\tau_{x,y,z}$ are the damping times of the transverse and longitudinal coordinates. The factors, R_i , are uncorrelated Gaussian distributed random numbers with the average $\langle R_i \rangle = 0$ and the standard deviation of $\langle R_i R_j \rangle = 1$ for $i=j$ and otherwise 0. The damped one-turn matrix, R_d , is simply given by the undamped matrix, R , multiplied by the corresponding damping factors and the diffusion matrix is diagonal with the elements:

$$D(1,1) = 2T_0/\tau_x \cdot \epsilon_{x_0} \cdot \beta_x, \quad D(2,2) = 2T_0/\tau_x \cdot \epsilon_{x_0}/\beta_x,$$

$$D(3,3) = 2T_0/\tau_y \cdot \epsilon_{y_0} \cdot \beta_y, \quad D(4,4) = 2T_0/\tau_y \cdot \epsilon_{y_0}/\beta_y,$$

$$D(5,5) = 2T_0/\tau_z \epsilon_{z_0} \cdot \beta_z, \text{ and } D(6,6) = 2T_0/\tau_z \cdot \epsilon_{z_0}/\beta_z.$$

At the observation point, the β -functions are β_x and β_y and we assume that $\alpha_x = \alpha_y = 0$ at this point. Without vertical bends the vertical emittance, ϵ_{y_0} , will be zero, ϵ_{z_0} and β_z are the longitudinal emittance and the longitudinal β -function [10]. In this approach the diffusion matrix is obtained by integrating the curly H-function over all horizontally bending dipoles with the help of known analytical functions [11], and the damping rates are given by the synchrotron integrals [11], all these parameters are calculated with the uncoupled lattice.

Solution of the mapping equation:

The equation $\Sigma_{s_0} = R_d \cdot \Sigma_{s_0} R_d^t + D_{s_0}$ can be written as [3]:

$$\Sigma_{s_0}(i,j) = \sum_{i',j'=1}^6 R_d(i,i') \cdot R_d(j,j') \cdot \Sigma_{s_0}(i',j') + D_{s_0}(i,j)$$

Following Ohmi, et al., one can create a vector, \vec{V} , composed of all 21 second-order moments of the Σ -matrix lined up and a similar vector, \vec{D} , constructed out of the 21 elements of the symmetric diffusion matrix, $D_{s_0}(i,j)$:

$$\vec{V} = (\langle xx \rangle, \dots, \langle x\delta \rangle, \langle x'x' \rangle, \dots, \langle x'\delta \rangle, \dots, \langle z, z \rangle, \langle z, \delta \rangle, \langle \delta\delta \rangle)^T, \text{ and:}$$

$$\vec{D} = (D_{s_0}(1,1), \dots, D_{s_0}(1,6), \dots, D_{s_0}(5,5), D_{s_0}(5,6), D_{s_0}(6,6), \dots)^T.$$

With the 21x21-matrix, A :

$$A(i,j) = \sum_{i',j'=1}^6 R_d(i,i') \cdot R_d(j,j'),$$

the equation $\Sigma_{s_0} = R_d \cdot \Sigma_{s_0} R_d^t + D_{s_0}$ can now be written in the following form:

$$\vec{V} = A \vec{V} + \vec{D}.$$

The solution for the 21 elements of the \vec{V} -vector is obtained by matrix inversion:

$$\vec{V} = -(A - I)^{-1} \cdot \vec{D},$$

with the identity matrix: $I = \begin{pmatrix} 1 & \dots & 0 \\ \vdots & \ddots & \vdots \\ 0 & \dots & 1 \end{pmatrix}$.

RESULTS

In the comparison of the three approaches, it is assumed that all magnetic elements are at their design location and that the closed orbit passes through the center of all magnets. Coupling is only created by skew quadrupole magnets centered on the nominal closed orbit which can be placed at dispersive and non-dispersive locations. For the numerical comparison, 16-fold linear optics were calculated based on the achromatic double bend lattice of the BESSY II storage ring with 240 m circumference. In the simulation, the 32 dipoles have been assumed to possess variable gradients to test the results for unequal transverse damping times. As mentioned, we are interested in observable quantities and we define the apparent emittance, E_x and E_y , as given by their coupling dependent moments and the three different approaches:

$$E_x = \sqrt{\langle xx \rangle \cdot \langle x'x' \rangle - \langle xx' \rangle \cdot \langle xx' \rangle}$$

$$E_y = \sqrt{\langle yy \rangle \cdot \langle y'y' \rangle - \langle yy' \rangle \cdot \langle yy' \rangle}.$$

A typical result of the simulations is shown in Fig. 2, where two quadrupole families are varied in such a way as to change dominantly the horizontal tune. A single skew quadrupole is used in this calculation with the strength normalized by $1/\sqrt{\beta_x \cdot \beta_y}$, with the beta functions, β_x , β_y , at the position of this magnet. The coupling element is placed either at a location without dispersion (shown in black) or with small or large dispersion (in color). For all three cases the coupling strength for the Q_x - Q_y -resonance is the same.

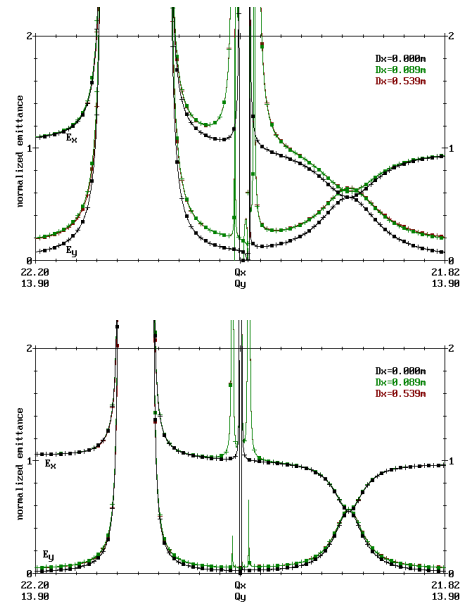


Figure 2: Normalized horizontal and vertical “emittance” as a function of the working point. The tunes at the start and the end of the scan are indicated on the horizontal axis. The coupling strength at the top is twice as strong as at the bottom. Results from Ohmi’s mapping approach are shown as squares, Chao’s results are represented by crosses, and the outcome of the mapping based on Hirata and Ruggiero is shown as solid lines.

The agreement between the three theoretical approaches for moderate strength of the coupling is very good, and shows, that the simplified modeling of the radiation effects yields valid results. The impact on the $Q_x \pm Q_y$ -resonance depends on the coupling to the longitudinal plane determined through the value of the horizontal dispersion function at the location of the skew quadrupole magnet.

As expressed in [3], predictions of Chao's SLIM approach differ from the correct mapping results for very small coupling strength and a linewidth dominated by the damping times. This is shown in Fig. 3, where the emittances on the difference and sum resonance, $Q_x \pm Q_y = \text{integer}$, are presented as a function of the normalized skew quadrupole strength for dipoles with and without transverse gradient, top and bottom of Fig. 3. If the coupling is created in a non-dispersive location, shown in black, then horizontal and vertical emittance remain the same even for very strong coupling. Their splitting in this region stems from the admixture of longitudinal emittance to the transverse planes which is different if also the horizontal dispersion is coupled to the vertical plane. The agreement between the simple and the full envelope mapping approach is evident.

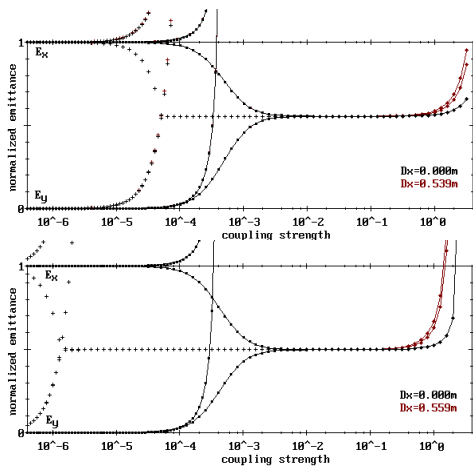


Figure 3: Normalized emittance as a function of coupling strength on the sum and difference resonance with and without dipole gradients (top and bottom). The sum-resonance leads to an enlargement of both transverse emittances which occurs at the same coupling strength because a single skew quadrupole magnet was used in the simulation. It takes a certain coupling strength to overcome the damping and diffusion from the emission of radiation and to produce a noticeable resonance excitation. With very strong coupling the emittance will blow up to infinity due to the overlap with the deadly sum-resonance. Symbols as in Fig. 2 and results of the simple mapping approach are shown as a solid line. Above a coupling strength of $5 \cdot 10^{-3}$, Chao's and Ohmi's results overlap and symbols appear as diamonds.

Based on the mapping results and with moderate coupling strength, the emittances near the difference coupling resonance can be written as:

$$\frac{\epsilon_y}{\epsilon_0} = \frac{4|C|^2 \sqrt{l_x l_y} (1 + \tau_y / \tau_x)}{4|C|^2 \sqrt{l_x l_y} \frac{(\tau_x + \tau_y)^2}{\tau_x \tau_y} + (T_0 / \tau_x + T_0 / \tau_y)^2 + (2\pi \Delta Q)^2}, \text{ and:}$$

$$\frac{\epsilon_x}{\epsilon_0} = \frac{4|C|^2 \sqrt{l_x l_y} (1 + \tau_y / \tau_x) + (T_0 / \tau_x + T_0 / \tau_y)^2 + (2\pi \Delta Q)^2}{4|C|^2 \sqrt{l_x l_y} \frac{(\tau_x + \tau_y)^2}{\tau_x \tau_y} + (T_0 / \tau_x + T_0 / \tau_y)^2 + (2\pi \Delta Q)^2}. C \text{ is the}$$

slightly modified complex coupling strength:

$$C(s_0) = \phi ds \frac{1}{B\rho} \frac{\partial B_x}{\partial x}(s) \cdot \sqrt{\beta_x(s)\beta_y(s)} \cdot e^{i(\mu_x(s) - \mu_y(s))}.$$

T_0 is the revolution time and $\Delta Q = Q_x - Q_y - n$, $n \in N$. With $|C| > 0$, the result for the full width at half maximum, FWHM, of the vertical resonance curve is:

$$\Delta Q_{FWHM} = \frac{1}{\pi} \sqrt{4 \cdot |C|^2 \sqrt{l_x l_y} \cdot \frac{(\tau_x + \tau_y)^2}{\tau_x \tau_y} + (T_0 / \tau_x + T_0 / \tau_y)^2}.$$

The above three formulas assume that the initial vertical emittance is zero and that the invariant emittance is ϵ_0 . The last term adds a small contribution to the line width from the finite damping time of the transverse single particle motion. This is shown in Fig. 4 where the results of mapping simulations are presented in comparison with the above approximate formulas which do not take into account the coupling with the longitudinal plane.

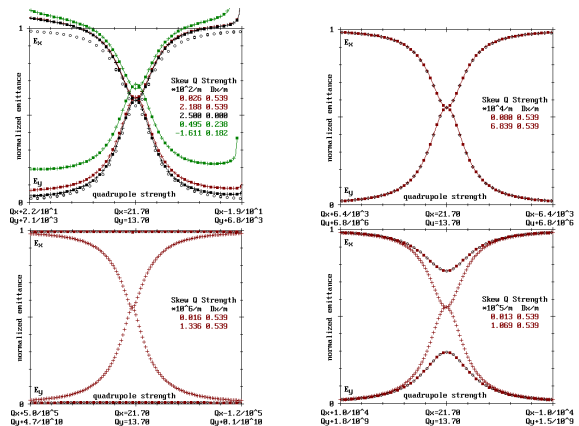


Figure 4: comparison of exact and approximate solutions for the line shape of the difference resonance as a function of the working point and coupling strength which becomes smaller in the clockwise direction. Results with the new formula are shown as black circles and do agree with the mapping results, especially if only the transverse planes are coupled. Symbols as in Fig. 2.

Note, that moment mapping is based on equilibrium and cannot describe the correct development of the emittances over time. Usually, this is not a serious problem since skew gradient or other coupling errors in a storage ring are static and we observe only the equilibrium situation anyway.

SUMMARY

The simplified treatment of radiation can be used to find an analytical formula for the emittance close to the linear difference coupling resonance in a region where coupling competes with damping and diffusion and the Hamiltonian approach is not applicable.

REFERENCES

- [1] G. Guignard, “Betatron coupling and related impact of radiation”, *Phys. Rev. E*, vol. 51, p. 6104, 1995.
- [2] K. Hirata, F. Ruggiero, “Treatment of Radiation for Multiparticle Tracking in Electron Storage Rings”, *Part. Acc.*, vol. 28, pp. 137-142, 1990.
- [3] K. Ohmi *et al.*, “From the Beam-Envelope Matrix to Synchrotron-Radiation Integrals”, *Phys. Rev. E*, vol. 49, p. 751, 1994.
- [4] A. Chao, “Evaluation of Beam Distribution Parameters in an Electron Storage Ring”, *J. Appl. Phys.*, vol. 50, p. 595, 1979.
- [5] A. Xiao, L. Emery, V. Sajaev, and B. X. Yang, “Experience with Round Beam Operation at the Advanced Photon Source”, in *Proc. IPAC'15*, Richmond, VA, USA, May 2015, pp. 562-564.
- [6] Y. Hidaka, W. X. Cheng, Y. Li, T. V. Shaftan, and G. M. Wang, “Round Beam Studies at NSLS-II”, in *Proc. IPAC'18*, Vancouver, Canada, Apr.-May 2018, pp. 1529-1532.
- [7] T. Zhang, X. Huang, “Off-axis injection for storage rings with full coupling”, *Phys. Rev. ST Accel. Beams*, vol. 21, p. 084002, 2018.
- [8] A. W. Chao, M.J. Lee, in “Particle distribution parameters in an electron storage ring”, *J. Appl. Phys.*, vol. 47, p. 4453, 1976
- [9] A. Wolski, “Low Emittance Machines – Emittance Computation and Tuning in Coupled Lattices”, presented at CERN Accelerator School, Daresbury, UK, 2007.
- [10] K. Hirata, *et al.*, in “A Symplectic Beam-Beam Interaction with Energy Exchange”, *Part. Acc.*, vol. 40, pp. 205-228, 1993.
- [11] X.J. Deng, *et al.*, “Courant-Snyder formalism of longitudinal dynamics”, *Phys. Rev. Accel- Beams*, vol. 24, p. 094001, 2021.
- [12] R.H. Helm, M.J. Lee, P.L. Morton, and M. Sands, “Evaluation of synchrotron radiation integrals”, *IEEE Trans. Nucl. Sci.*, vol. 20, p. 900, 1973.